Increased Air Temperature during Simulated Autumn Conditions Impairs Photosynthetic Electron Transport between Photosystem II and Photosystem I[1][OA]

Florian Busch, Norman P.A. Hüner, and Ingo Ensminger*

Department of Biology and the BIOTRON, University of Western Ontario, London, Ontario, Canada N6A 5B7 (F.B., N.P.A.H., I.E.); Institute of Chemistry and Dynamics of the Geosphere ICG-II, Phytosphere, Research Center Jülich, 52425 Juelich, Germany (F.B.); and Department of Forest Ecology, Forest Research Institute Baden-Wuerttemberg, 79100 Freiburg, Germany (I.E.)

Changes in temperature and daylength trigger physiological and seasonal developmental processes that enable evergreen trees of the boreal forest to withstand severe winter conditions. Climate change is expected to increase the autumn air temperature in the northern latitudes, while the natural decreasing photoperiod remains unaffected. As shown previously, an increase in autumn air temperature inhibits CO_2 assimilation, with a concomitant increased capacity for zeaxanthin-independent dissipation of energy exceeding the photochemical capacity in *Pinus banksiana*. In this study, we tested our previous model of antenna quenching and tested a limitation in intersystem electron transport in plants exposed to elevated autumn air temperatures. Using a factorial design, we dissected the effects of temperature and photoperiod on the function as well as the stoichiometry of the major components of the photosynthetic electron transport chain in *P. banksiana*. Natural summer conditions (16-h photoperiod/22°C) and late autumn conditions (8-h photoperiod/7°C) were compared with a treatment of autumn photoperiod with increased air temperature (SD/HT: 8-h photoperiod/22°C) and a treatment with summer photoperiod and autumn temperature (16-h photoperiod/7°C). Exposure to SD/HT resulted in an inhibition of the effective quantum yield associated with a decreased photosystem II/photosystem I stoichiometry coupled with decreased levels of Rubisco. Our data indicate that a greater capacity to keep the primary electron donor of photosystem I (P700) oxidized in plants exposed to SD/HT compared with the summer control may be attributed to a reduced rate of electron transport from the cytochrome b_6f complex to photosystem I. Photoprotection under increased autumn air temperature conditions appears to be consistent with zeaxanthin-independent antenna quenching through light-harvesting complex II aggregation and a decreased efficiency in energy transfer from the antenna to the photosystem II core. We suggest that models that predict the effect of climate change on the productivity of boreal forests must take into account the interactive effects of photoperiod and elevated temperatures.

Cold hardening in conifers is a physiological process that includes the cessation of growth and long-term changes in metabolism. In evergreen trees of the boreal forest, this process is triggered by short days and potentiated by low temperature (Weiser, 1970; Christersson, 1978; Bigras et al., 2001; Li et al., 2002; Beck et al., 2004; Puhakainen et al., 2004). One of the major challenges for overwintering evergreen conifers like *Pinus banksiana* is balancing the photosynthetic electron transport rate with the rate of consumption of reductant by metabolism (Busch et al., 2007). This is especially important since evergreen conifers retain a substantial amount of chlorophyll throughout the winter and hence continue to absorb light, while at the same time the short photoperiod-, low temperature-induced, down-regulated metabolism is not able to utilize the absorbed energy. Light capture and energy utilization are regulated in a coordinated manner to prevent oxidative damage to the photosynthetic apparatus. Energy balance, defined as photostasis (Öquist and Huner, 2003), is achieved by reorganization of the photosynthetic machinery, including changes in antenna size and organization, adjustments of protein and chlorophyll concentrations, and a range of alternative energy dissipation pathways (Demmig-Adams et al., 1996; Asada, 1999; Öquist and Huner, 2003; Ensminger et al., 2004, 2006; Horton et al., 2005; Sveshnikov et al., 2006; Rumeau et al., 2007).

Under conditions in which more light energy is absorbed than can be utilized, an increase in nonradiative dissipation can be observed as nonphotochemical quenching of chlorophyll fluorescence (NPQ).

[1] This work was supported by a Marie-Curie Fellowship of the European Union (PhysConFor, contract no. MOIF–CT–2004-002476) to I.E. and by grants from the Natural Sciences and Engineering Research Council of Canada and the Canada Foundation for Innovation to N.P.A.H.

* Corresponding author; e-mail ingo.ensminger@ctp.uni-freiburg.de.

The author responsible for distribution of materials integral to the findings presented in this article in accordance with the policy described in the Instructions for Authors (www.plantphysiol.org) is: Ingo Ensminger (ingo.ensminger@ctp.uni-freiburg.de).

[OA] Open Access articles can be viewed online without a subscription.

www.plantphysiol.org/cgi/doi/10.1104/pp.108.117598

NPQ is linked to the deepoxidation of violaxanthin to zeaxanthin via the xanthophyll cycle (Demmig-Adams et al., 1996). It consists of different components that are distinguished by their characteristics in induction and relaxation kinetics (Müller et al., 2001). The major component of NPQ is q_E, which is dependent on the pH gradient across the thylakoid membrane. It builds up and relaxes rapidly within seconds to minutes. A more sustained quenching mode is represented by q_I, which relaxes more slowly and is related to photoinhibition of photosynthesis (Müller et al., 2001).

Not all of the energy absorbed in excess is dissipated in the antenna. Electrons in excess are also used by photorespiration (Wingler et al., 2000) or to produce ATP via cyclic electron flow (Rumeau et al., 2007). Excitation pressure (Huner et al., 1998) can be reduced by transferring electrons to oxygen via the water-water cycle (Asada, 2000) or via chlororespiration through the plastid terminal oxidase (PTOX; Peltier and Cournac, 2002; Rumeau et al., 2007). Aside from being upregulated under stress conditions (Streb et al., 2005; Quiles, 2006), PTOX is involved in carotenoid biosynthesis (Carol et al., 1999). However, overexpression of PTOX did not result in an increased resistance to photoinhibition in Arabidopsis (*Arabidopsis thaliana*); therefore, it has been suggested that PTOX cannot be considered a significant protective safety valve in fully expanded leaves of Arabidopsis (Rosso et al., 2006). Intersystem electron transport is dependent on the diffusion of plastoquinone (PQ) between PSII and the cytochrome (Cyt) b_6f complex (Haehnel, 1984). Plastocyanin (PC) may also regulate electron flux under conditions in which carbon assimilation is limited (Schöttler et al., 2004). It has been demonstrated that only a minor fraction of PC, located in the outer regions of grana, is used to facilitate rapid electron transfer between the Cyt b_6f complex and PSI (Kirchhoff et al., 2004). This electron transfer can be severely inhibited by an impairment of PC diffusion due to proteins protruding into the luminal diffusion space or a reduction in the volume of the thylakoid lumen (Haehnel, 1984).

The northern latitudes, habitat of tundra and boreal forests, have experienced a dramatic increase in surface air temperature over the past decades, with increases observed especially in the winter, and this trend is expected to continue (ACIA, 2005; IPCC, 2007). Given these changes in the arctic climate, the length of the growing season is likely to increase by 20 to 30 d by 2080 (ACIA, 2005) and thereby improve the productivity of northern hemisphere forests (White et al., 2000; Saxe et al., 2001). However, it was recently shown that boreal evergreen conifers might not be able to fully exploit an extended growing season, as a result of either an earlier onset of spring conditions (Slot et al., 2005; Ensminger et al., 2008) or prolonged warmer temperatures during autumn (Busch et al., 2007). Under simulated increased autumn air temperatures in *P. banksiana*, carbon assimilation rates were reduced, with a concomitant increase in NPQ of absorbed energy. However, the energy-quenching mechanism was inconsistent with the well-described zeaxanthin- and PsbS-dependent dissipation pathways for photoprotection (Busch et al., 2007). A model was proposed whereby antenna quenching was dependent on the deepoxidation state of the pool of xanthophyll cycle pigments as well as on the protonation of light-harvesting complex II (LHCII), affecting the degree of LHCII aggregation (Horton et al., 2005; Busch et al., 2007). To test this model, we assessed the effects of elevated autumn air temperatures in *P. banksiana* on photosystem stoichiometry, antenna quenching, xanthophyll cycle activity, and intersystem electron transport. As controls, we used two treatments representing, first, natural summer conditions (LD/HT: 16-h photoperiod/22°C) and, second, late autumn conditions (SD/LT: 8-h photoperiod/7°C). To simulate increased autumn air temperatures, a treatment with autumn photoperiod and summer temperature (SD/HT: 8-h photoperiod/22°C) was compared with the two controls. In addition, a second experimental treatment with summer photoperiod and autumn temperature (LD/LT: 16-h photoperiod/7°C) was used to separate the effects of photoperiod and temperature.

RESULTS

Effects of Photoperiod and Temperature on the Polypeptide Composition of the Photosynthetic Apparatus

Regardless of photoperiod, Lhcb1 levels in LD/HT and SD/HT plants were about 50% lower than in plants exposed to either LD/LT or SD/LT (Fig. 1A), which is consistent with previous results (Busch et al., 2007). The abundance of the PSII reaction center polypeptide, PsbA, was highest in the summer control (LD/HT) and decreased to 20% ± 4% of that amount in the autumn control (SD/LT; Fig. 1B). The amount of PsbA in *P. banksiana* exposed to SD/HT conditions was intermediate to that of the two control treatments (65% ± 9% of LD/HT) and attained the lowest levels in LD/LT plants (9% ± 3%). The reaction center polypeptides of PSI (PsaA/B) also reached the highest amounts in LD/HT plants, and the levels in SD/LT plants were less than half of that (45% ± 9%). In plants exposed to SD/HT, however, PsaA/B did not decrease, and the amount was comparable to that in the summer control (LD/HT; 108% ± 7%). As for PsbA, the lowest amounts of PsaA/B were also detected in LD/LT plants (18% ± 2%; Fig. 1C). Cyt *f*, a protein linking the electron transport chain between PSII and PSI, and RbcL, the large subunit of the Calvin cycle protein Rubisco, followed a similar pattern as PsbA. For Cyt *f*, the highest amounts were detected in the summer control (LD/HT) and decreased to 90% ± 17% in the autumn control (SD/LT; Fig. 1D). In SD/HT plants, the amount of Cyt *f* was 85% ± 15% of LD/HT plants and the lowest amount again was detected in LD/LT plants

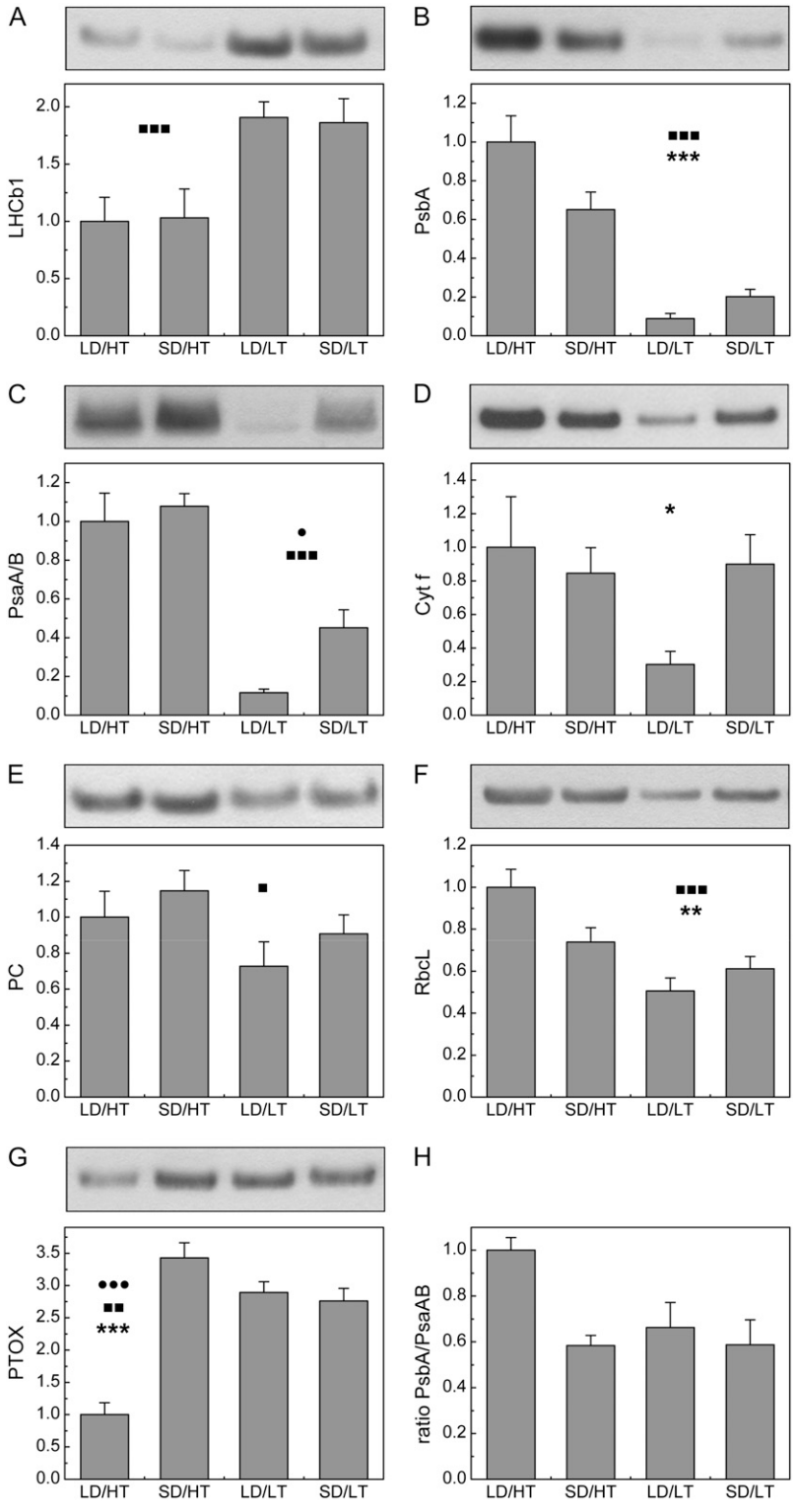

Figure 1. The effect of daylength and temperature on the expression levels of key proteins of the photosynthetic electron transport chain in needles of *P. banksiana*. The average optical density of the LD/HT treatment was arbitrarily scaled to 1. Typical bands from the original western blots, loaded on an equal protein basis, are shown above the values. Each value represents the average of $n = 8 \pm$ SE biological replicates. Two-way ANOVA indicates statistically significant differences due to daylength, temperature, or an interactive effect of both factors. ●, ■, and * indicate significant differences due to daylength, temperature, and their interactive effect, respectively. One symbol, $P < 0.05$; two symbols, $P < 0.01$; three symbols, $P < 0.001$.

(30% ± 8%). RbcL in the autumn control (SD/LT; 61% ± 6%) was significantly reduced compared with the summer control (LD/HT; Fig. 1F). In plants exposed to SD/HT, the amount of RbcL (74% ± 7%) was intermediate between the summer and the autumn controls, and the lowest amounts were observed under LD/LT conditions (51% ± 6%). The amount of PC, which transfers electrons from the Cyt b_6f complex to PSI, was comparable between the two control treatments, with the autumn control (SD/LT) reaching

91% ± 11% of the summer control (LD/HT; Fig. 1E). In contrast to the other components of the photosynthetic apparatus, the amount of PC increased to 115% ± 11% in SD/HT plants compared with the summer control (LD/HT). The lowest amounts were detected in LD/LT plants (73% ± 14%). PTOX responded to exposure to the autumn control conditions (SD/LT) by increasing protein content to 276% ± 20% relative to the summer control (LD/HT). Similar increases were detected for plants exposed to LD/LT conditions (289% ± 17%). However, when *P. banksiana* was treated to SD/HT conditions, PTOX content (343% ± 24%) was stimulated to the greatest extent (Fig. 1G).

Effects of Photoperiod and Temperature on Photosynthetic Pigments

To test the validity of the quenching mechanism in the model proposed by Busch et al. (2007), we tested the activity of the xanthophyll cycle. Figure 2A shows the deepoxidation status (DEPS) of the xanthophyll cycle pigments for the four treatments in response to short-term (2-h) exposure to various light intensities. All treatments show a saturation of DEPS at light intensities of 800 μmol photons m^{-2} s^{-1} or more. Major differences between the four treatments can be seen in the dark-adapted state and at light intensities ranging up to 500 μmol photons m^{-2} s^{-1}. In the summer control (Fig. 2A, black circles), DEPS was considerably lower than in the autumn control (Fig. 2A, white squares). The highest DEPS at all light intensities was detected in plants exposed to LD/LT conditions (Fig. 2A, white squares), which reflects the fact that most of the xanthophyll cycle pigments were found in the form of zeaxanthin. Thus, the results for summer (LD/HT) and autumn (SD/LT) controls as well as for plants exposed to LD/LT indicate that *P. banksiana* exhibits a normal xanthophyll cycle. Interestingly, DEPS in plants exposed to SD/HT was substantially lower than even the summer control (Fig. 2A, black squares), reaching only about one-third of LD/HT in the dark-adapted state.

The total size of the xanthophyll cycle pigment pool exhibited only minimal changes between treatments and was only dependent on photoperiod, not on temperature (Fig. 2B). Therefore, decreased levels of DEPS also indicate decreased total amounts of zeaxanthin, as the overall amount of xanthophyll cycle pigments did not increase. In SD/HT- and SD/LT-exposed plants, the pool size was 13% less than in LD/HT plants. LD/LT plants, which showed the highest DEPS, had 23% more xanthophyll cycle pigments than the summer control and about 40% more than the short-day treatments (Fig. 2B).

β-Carotene levels were equivalent in the summer and autumn controls (Fig. 2C). However, under SD/HT conditions, we observed about 50% higher levels of β-carotene than in either the summer or autumn control treatments as well as in plants exposed to LD/LT conditions.

Effects of Photoperiod and Temperature on PSII and PSI Function

PSII Function

Chlorophyll fluorescence was used to probe PSII function. In accordance with the abundance of PsbA (Fig. 1B), photochemical efficiency (F_v/F_m) was highest in the summer control (LD/HT; 0.77 ± 0.01). In contrast, the autumn control plants were photoinhibited and showed a severely reduced F_v/F_m (SD/LT; 0.15 ± 0.02), similar to that of plants exposed to LD/LT conditions (0.08 ± 0.01). However, under increased autumn air temperatures, we observed minimal photoinhibition (SD/HT; 0.70 ± 0.02). Clearly, a low-temperature growth regime had a significant effect on maximum photochemical efficiency, whereas the effect of photoperiod appeared to be minimal.

To examine this in more detail, we assessed the effects of growth regime on the fluorescence induction curves. In all four treatments, fluorescence yield (F_s) initially increased when the light was turned on and subsequently decreased to steady-state levels (Fig. 3). In the autumn control as well as in plants exposed to LD/LT, changes in the fluorescence yield were minimal and F_s reached initial minimal fluorescence (F_0) levels within about 1 min. These results are consistent with those of F_v/F_m. Consistent with the F_v/F_m data, both summer control (LD/HT) and SD/HT plants exhibited significant increases in F_s upon exposure to actinic light. However, F_s was rapidly quenched within the first minute to levels that were lower than F_0. The extent of this quenching appeared to be greater in plants exposed to SD/HT conditions than in the summer control (LD/HT). This effect was reversible when the light was switched off. After turning off the actinic light, a very rapid recovery of F_s close to F_0 levels within minutes was observed in SD/HT plants but not in any other treatment. This rate of recovery of F_s was enhanced by applying far-red (FR) light (Fig. 3, inset).

Since there appeared to be a considerable effect of both growth temperature and photoperiod on fluorescence quenching, we examined the effects of growth regime on the light response curves for fluorescence quenching parameters, the redox state of PSII, as well as the effective quantum yield of PSII (Fig. 4). Plants grown at low temperature exhibited a significantly lower amount of NPQ than plants grown at high temperature, irrespective of photoperiod (Fig. 4A). At light intensities up to 800 μmol photons m^{-2} s^{-1}, NPQ was slightly higher in SD/HT than in LD/HT plants. Under low to moderate light intensities, NPQ responded more strongly to an increase in light intensity in SD/HT than in LD/HT plants (Fig. 4A) and thus showed a 1.55-fold maximum quantum efficiency for NPQ (LD/HT, 8.5 ± 1.5 × 10^{-3} NPQ per μmol photons m^{-2} s^{-1}; SD/HT, 13.2 ± 2.4 × 10^{-3}), determined as the initial slope of the light saturation curve for NPQ. In plants treated with low temperature, maximum quan-

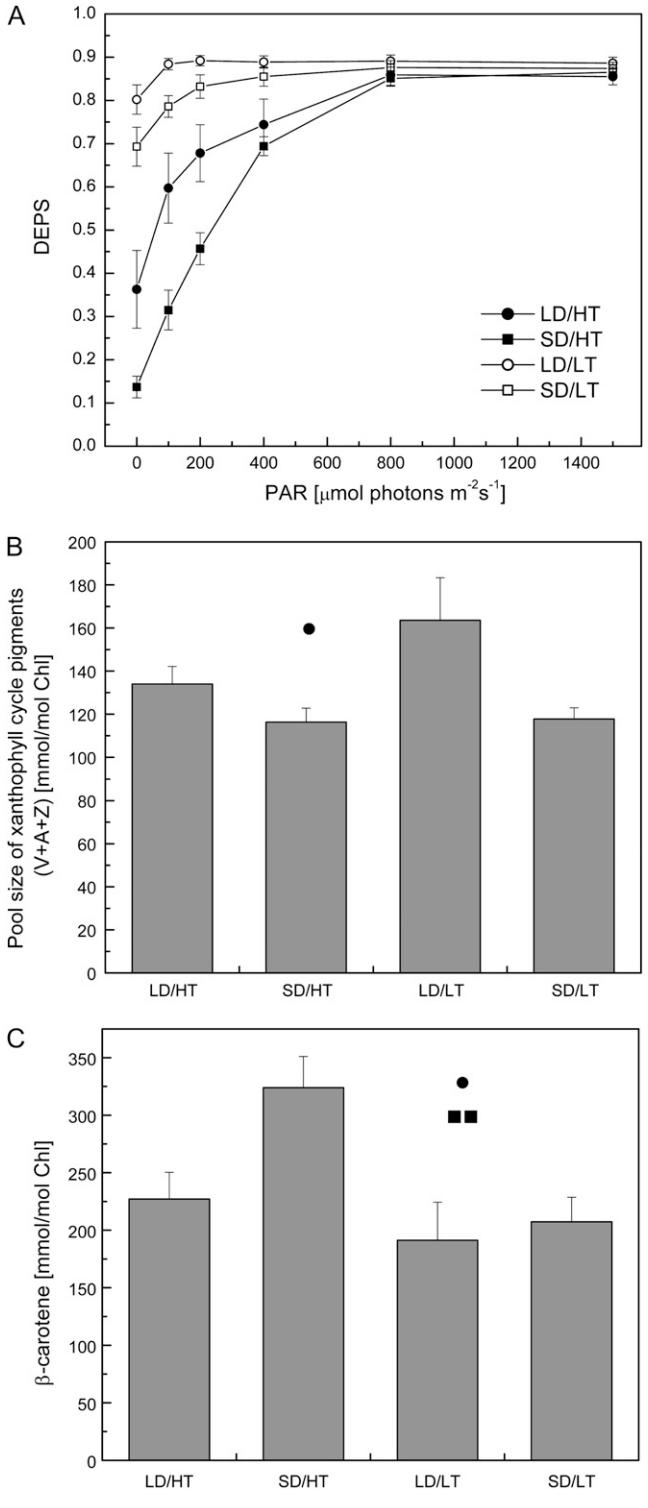

Figure 2. The effect of daylength and temperature on the composition of photosynthetic pigments in needles of *P. banksiana*. A, DEPS of the xanthophyll cycle pigments in response to photosynthetically active radiation (PAR), calculated as (0.5A + Z)/(V + A + Z). Needles were exposed to the corresponding light intensity for 2 h before harvesting. B, Total pool size of xanthophyll cycle pigments (V + A + Z) per total chlorophyll. C, Amount of β-carotene per total chlorophyll. Each data point represents the average of $n = 8 \pm$ SE biological replicates. ●, ■, and * indicate significant differences due to daylength, temperature, and their interactive effect, respectively. One symbol, $P < 0.05$; two symbols, $P < 0.01$.

tum efficiency of NPQ was reduced by 6- to 9-fold irrespective of photoperiod (LD/LT, $1.7 \pm 0.1 \times 10^{-3}$ NPQ per μmol photons m^{-2} s^{-1}; SD/LT, $1.5 \pm 0.3 \times 10^{-3}$). These trends were confirmed by assessing antenna quenching measured as q_0 (Fig. 4B).

Excitation pressure ($1 - q_P$), a measure of the reduction state of PSII reaction centers, was lowest in the summer control (LD/HT) and highest in the autumn control (SD/LT) and in plants exposed to LD/LT (Fig. 4C). Over the whole range of light intensities tested, SD/HT plants showed a $1 - q_P$ higher than the summer control but lower than the autumn control. Thus, although low temperature had the greatest effect on excitation pressure, combining summer temperatures with a short photoperiod significantly increased the proportion of closed PSII reaction centers.

Figure 4D depicts the effective quantum yield of PSII (F_v'/F_m'). Summer control (LD/HT) plants showed the highest yield across all light intensities. In the autumn control (SD/LT) as well as in LD/LT plants, F_v'/F_m' was substantially decreased. However, changing only the photoperiod from LD/HT to SD/HT caused a decrease in F_v'/F_m' to about half of the summer control value (Fig. 4D).

PSI Function

The extent of FR light-induced absorbance change was used to estimate PSI function in vivo (Klughammer and Schreiber, 1991; Ivanov et al., 1998). Both the autumn control (SD/LT) and plants exposed to LD/LT exhibited a 30% to 50% lower relative amount of FR-oxidized $P700^+$, estimated as absorbance change around 820 nm ($\Delta A_{820}/A_{820}$), than the summer control (LD/HT; Fig. 5A). This is consistent with the levels of PsaA/B detected in these samples (Fig. 1C). However, under SD/HT conditions, we observed an increase of 67% in the $\Delta A_{820}/A_{820}$ signal compared with summer LD/HT conditions, which could not be accounted for by higher levels of PsaA/B (Fig. 1C).

The summer control (LD/HT) showed the shortest half-time for $P700^+$ reduction after the FR light source was turned off (Fig. 5B). The half-time of the autumn control (SD/LT) was 61% higher, which is an indication of lower PSI cyclic electron transport (Maxwell and Biggins, 1976), compared with the summer control (LD/HT). Under SD/HT, we observed an increase in the half-time of $P700^+$ reduction by 91% relative to LD/HT. The slowest $P700^+$ reduction was detected in LD/LT, with an increase of 182% compared with LD/HT. Clearly, exposure to both low temperature and a short photoperiod increased the half-time for dark reduction of $P700^+$ relative to summer control plants.

We found a clear temperature dependence in the pool size of electrons in the intersystem electron trans-

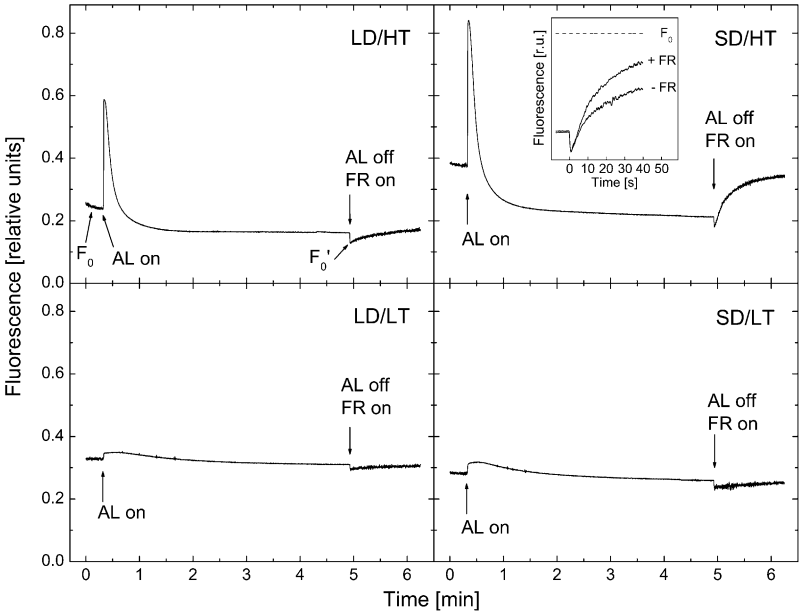

Figure 3. Fluorescence transients of *P. banksiana* needles grown under LD/HT, SD/HT, LD/LT, and SD/LT conditions. Dark-adapted needles were exposed to actinic light (AL) of 650 μmol photons m^{-2} s^{-1} for 4.5 min before the light was turned off and FR light was turned on. Traces are averages of five independent biological replicates. The inset shows the rate of fluorescence recovery during the first 40 s after turning off actinic light in SD/HT with and without applying FR light. Note that the fluorescence transients shown here do not result from saturating flash-induced fluorescence kinetics, as in Figure 4 (see "Materials and Methods" for further details).

port chain (e^-/P700), calculated as the area ratio of multiple-turnover to single-turnover flash (Fig. 5C). The intersystem electron pool size in the summer control (LD/HT) was about twice as large as that of either the autumn control or plants exposed to LD/LT. Plants exposed to SD/HT conditions exhibited a pool size similar to that of the summer control.

Energy Distribution between PSII and PSI

Changes in the PSII and PSI polypeptide content (Fig. 1, B and C) were also reflected in the 77 K fluorescence emission spectra (Fig. 6A). Shown are the averages of eight spectra for each treatment for all four treatments. Average spectra illustrate the emission obtained between 650 and 800 nm when excited at 436 nm, normalized to the emission of 685 nm. As expected, fluorescence maxima were detected at 685, 694, and 731 nm in the summer control (LD/HT; Fig. 6A, solid line), the first two representing emissions from the PSII core and the last from PSI (Krause and Weis, 1991). Under autumn control conditions (SD/LT), the amplitude of the long-wavelength fluorescence peak increased and the peak maximum was shifted from 731 to 723 nm. It is obvious from Figure 6A that the emission ratio of PSII to PSI strongly decreases in both the autumn control (SD/LT) and LD/LT plants compared with the summer control (LD/HT), reflecting the ratio in PsbA to PsaA/B polypeptide composition (Fig. 1H). However, in plants exposed to SD/HT conditions, the lower ratio of PsbA to PsaA/B polypeptides was not reflected in major changes in the ratio of PSII to PSI fluorescence emission.

In addition, the difference spectra between the autumn and summer controls (SD/LT − LD/HT) indicated a distinct peak at 676 nm (Fig. 6B). A similar peak at 676 nm was observed in the difference spectra between plants exposed to LD/LT and the summer control (LD/LT − LD/HT). Thus, exposure of *P. banksiana* to low temperature appears to cause a blue shift in the PSI emission at 731 nm (Fig. 6A) and enhanced fluorescence emission at 676 nm (Fig. 6B). Although exposure of plants to SD/HT caused a minimal blue shift in the PSI emission band at 731 nm, this did result in enhanced emission at 676 nm relative to the summer control, as observed in plants exposed to low temperature (Fig. 6B).

DISCUSSION

Exposure to SD/HT Conditions Alters the Structure and Composition of the Photosynthetic Apparatus, Causing Inhibition of Photosynthetic Electron Transport

P. banksiana is an important species in boreal evergreen forests. Global climate change measurements over the past decades indicate that the average surface air temperature has increased significantly, and this warming trend is predicted to continue (ACIA, 2005; IPCC, 2007). It has been suggested that this would lead to an increase in the growing season and, thus, enhance the productivity of the boreal forests. Changes in temperature and photoperiod are the predominant environmental signals used by conifers such as *P. banksiana* to induce the dormant state in the autumn and achieve cold hardiness, which is required by vegetative tissue and reproductive organs to survive boreal winter conditions. However, warming trends in the northern latitudes occur with no change in seasonal photoperiods. Recently, we reported that, contrary to expectations, increased autumn temperature combined with a normal, short autumn photoperiod (SD/HT) inhibits rather than enhances the photosyn-

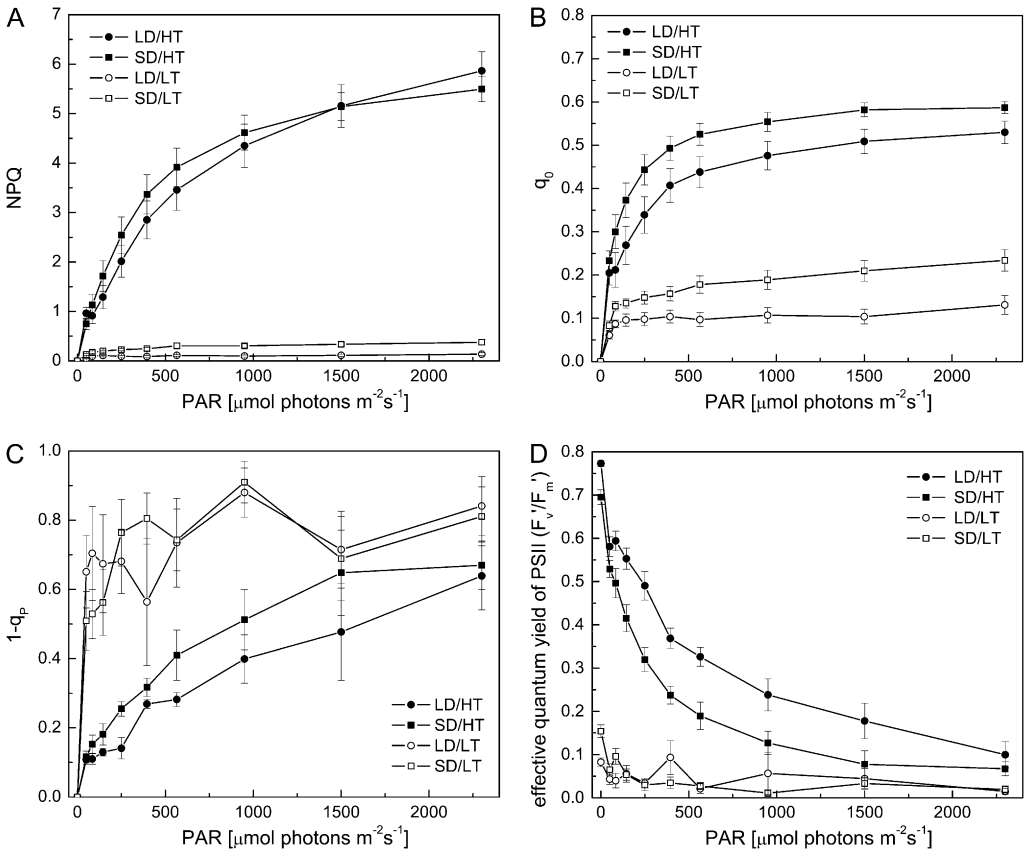

Figure 4. The effect of daylength and temperature on chlorophyll fluorescence parameters in response to photosynthetically active radiation (PAR). A, Light saturation curve for NPQ. B, Light saturation curve for antenna quenching (q_0). C, Estimated fraction of closed PSII reaction centers ($1 - q_P$). D, Effective quantum yield of PSII (F_v'/F_m'). All measurements were performed at growth temperature (22°C for LD/HT and SD/HT and 7°C for LD/LT and SD/LT) at the end of the night on dark-adapted seedlings. Each data point represents the average of $n = 6$ to 8 ± SE biological replicates.

thetic capacity of *P. banksiana*, measured as CO_2 assimilation (Busch et al., 2007). Here, we show that this inhibition of photosynthesis in plants exposed to SD/HT can be accounted for, at least in part, by a significant impairment of photosynthetic electron transport due to alterations in the structure and composition of the photosynthetic apparatus. First, by probing PSII function by chlorophyll *a* fluorescence, we observed that, relative to our summer control (LD/HT), exposure to SD/HT conditions inhibited the effective quantum yield (Fig. 4D), which was associated with increased excitation pressure, measured as $1 - q_P$ (Fig. 4C). Second, by probing the redox state of PSI by measuring $\Delta A_{820}/A_{820}$ (Fig. 5A), we observed that plants exposed to an autumn photoperiod but elevated temperatures (SD/HT) exhibited higher levels of $P700^+$ relative to the summer control (LD/HT). Since this was associated with lower levels of Rubisco but comparable levels of PsaA/B (Fig. 1, B and F), the greater capacity to keep P700 oxidized in SD/HT compared with LD/HT plants cannot be due to enhanced photosynthetic capacity, since CO_2 assimilation is inhibited (Busch et al., 2007). Although there appears to be a limitation on the acceptor side of PSI based on Rubisco levels (Fig. 1F) and CO_2 assimilation rates (Busch et al., 2007), there must be an even greater limitation on the donor side of PSI to account for this higher capacity to keep P700 oxidized in SD/HT versus LD/HT plants.

Where is the site of limitation in photosynthetic electron transport in plants grown in SD/HT conditions? The site of limitation is not k_1 (Fig. 7), since the quenching in the light (Fig. 3) and considerable $1 - q_P$ (Fig. 4C) indicate a buildup of a proton gradient due to PQ reduction, and there were no significant differences in either F_v/F_m or intersystem electron pool size (e^-/P700; Fig. 5C) in SD/HT plants compared with summer control plants (LD/HT). Assuming that Cyt b_6f is evenly distributed throughout grana and stroma (Albertsson, 2001), the diffusion distance for the reduced PQ is kept short and therefore is not likely to pose a major limitation on photosynthetic electron transport. The NAD(P)H dehydrogenase complex appears to be absent in pine chloroplasts (Wakasugi et al., 1994); therefore, it is unlikely that the stroma (k_2) contributes significantly to the PQ reduction. PTOX accumulation does not alleviate excitation pressure

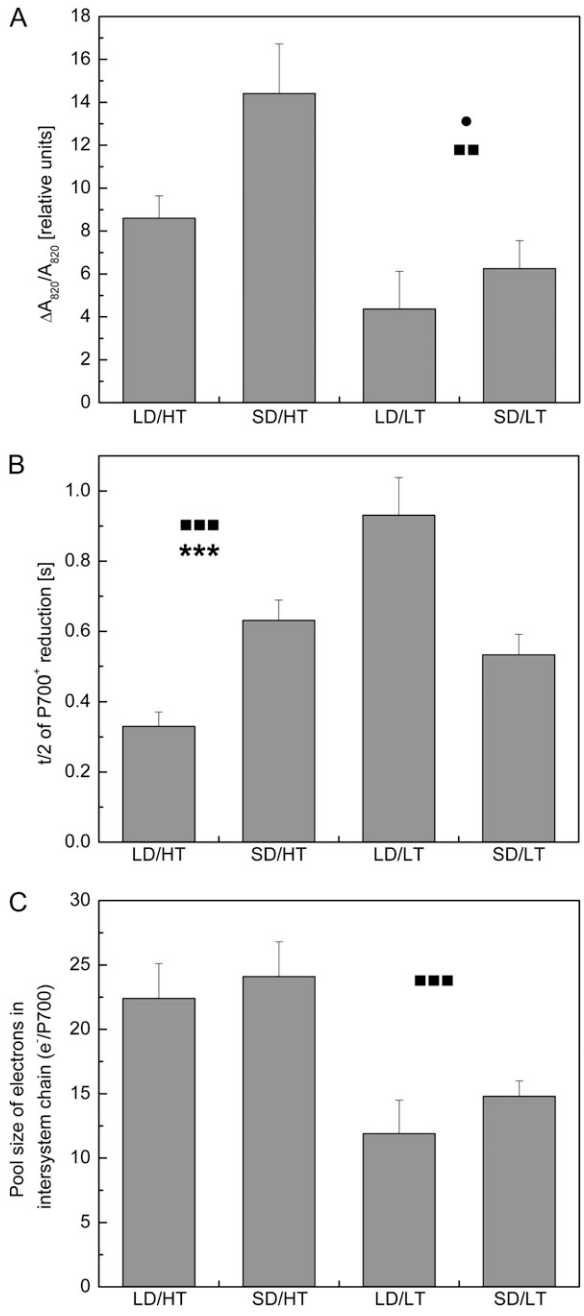

Figure 5. The effect of daylength and temperature on in vivo P700 parameters in *P. banksiana* needles grown under different daylength and temperature regimes. After a steady-state level of $P700^+$ was achieved under FR illumination, single-turnover and multiple-turnover pulses were applied. A, Steady-state oxidation of P700 ($\Delta A_{820}/A_{820}$). B, Reduction kinetics of $P700^+$ after the FR light was turned off (t/2). C, Effective intersystem electron pool size (e^-/P700). All measurements were performed at the growth temperature. Each data point represents the average of $n = 6$ to 8 ± SE biological replicates. ●, ■, and * indicate significant differences due to daylength, temperature, and their interactive effect, respectively. One symbol, $P < 0.05$; two symbols, $P < 0.01$; three symbols, $P < 0.001$.

under SD/HT conditions, making it unlikely for k_3 to be a major exit route for electrons. The limiting step is also not between PSI and the assimilation of CO_2 (k_5), given that high levels of $P700^+$ are associated with lower levels of Rubisco and reduced CO_2 assimilation rates (Busch et al., 2007). Because cyclic electron transport (k_6) is reduced, we suggest that the probable limitation in photosynthetic electron transport must be between Cyt b_6f and PSI (k_4; Fig. 7). This would be consistent with the observation that plants exposed to SD/HT conditions exhibited a greater quenching of F_s, which was rapidly relaxed either in the dark or by the addition of FR light to activate PSI (Fig. 3). Therefore, the rate-limiting step in the transfer of electrons from PSII to PSI would be the limitation in diffusion of PC. Diffusion of PC could be impaired by (1) a reduction of the lumen width (e.g. as a result of hyperosmotic stress; Cruz et al., 2001), (2) protruding proteins in the luminal diffusion space (Kirchhoff et al., 2004), or (3) a change in PC concentration or a greater spatial separation of PSII and PSI. Golding and Johnson (2003) proposed a model in which the spatial separation of PSII and PSI is exacerbated under unfavorable conditions due to a shift of active PSI from the grana margins to a separate pool in the stroma thylakoids, which would limit electron transfer between PSII and PSI. A situation in which the reduction of Cyt b_6f by PQ occurs faster than its reoxidation by PC, likely due to slow PC migration, has been reported in aging tobacco (*Nicotiana tabacum*) leaves (Schöttler et al., 2004).

LHCII Trimerization Facilitates Zeaxanthin-Independent Quenching of Excess Energy

The xanthophyll cycle generally plays a major role in the photoprotection of plants, and thermal dissipation of excess energy under high light is facilitated by zeaxanthin and antheraxanthin in the antenna of PSII (Adams et al., 2004). However, previous work has shown that the zeaxanthin-dependent pathway is not the dominant mechanism to dissipate excess energy in the antenna of SD/HT plants, and a model was proposed in which antenna quenching occurs by increased LHCII trimerization (Busch et al., 2007). Here, we provide functional evidence that plants exposed to SD/HT conditions exhibit enhanced antenna quenching compared with the summer control (LD/HT) when measured as q_{l0} (Fig. 4B). Furthermore, in vitro, the transition from monomeric to trimeric LHCII is characterized by an increase in 77 K fluorescence at 675 nm (Klimov, 2003; Wentworth et al., 2004). Our fluorescence difference spectra, obtained by subtracting the LD/HT trace from the traces of each treatment, show a peak at this wavelength, indicating an increase in the proportion of trimeric LHCII (Fig. 4B). This is in agreement with our previous observations based on nondenaturing SDS-PAGE, showing an increased ratio of trimeric to monomeric LHCII (Busch et al., 2007). We also observed a decrease of the peak at 694 nm relative to the peak at 685 nm (Fig. 6), which originates

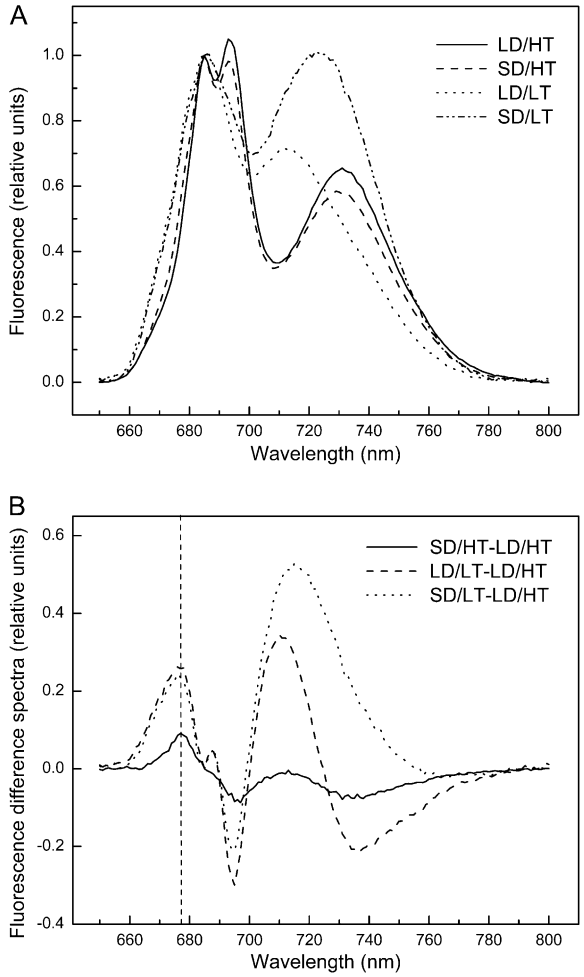

Figure 6. The effect of daylength and temperature on low-temperature (77 K) fluorescence emission properties in *P. banksiana* needles grown under different daylength and temperature regimes. A, Fluorescence emission spectra (excited at 436 nm) of the four different treatments. The spectra were normalized to the peak at 685 nm. Each trace represents the average of $n = 8$ independent biological replicates. B, Corresponding difference spectra SD/HT − LD/HT, LD/LT − LD/HT, and SD/LT − LD/HT. The chlorophyll concentration of all samples was 5 μg mL^{-1}.

from the PSII core and LHCII, respectively (Vandorssen et al., 1987; Krause and Weis, 1991). These results indicate that the efficiency of energy transfer from the antenna to the core is decreased in SD/HT compared with LD/HT and especially in the two low-temperature treatments. We suggest that, at least in SD/HT plants, this is due to a decrease in the relative amount of the minor LHC, as shown previously for Lhcb5 (Busch et al., 2007), the innermost LHC protein, connecting LHCII to the PSII core (Bossmann et al., 1997). We conclude that the trimerization of LHCII together with the uncoupling from the core may protect PSII from photodamage under conditions in which the capacity for CO_2 assimilation is suppressed.

Figure 2A shows that plants exposed to SD/HT have by far the lowest DEPS, yet the xanthophyll cycle is fully functional in all four treatments. Whereas in the two low-temperature treatments the xanthophyll pool is largely deepoxidized even in the dark, the two high-temperature treatments exhibit this behavior only under high irradiance. The lower DEPS in SD/HT compared with LD/HT plants is not due to a larger total pool size of the xanthophyll cycle pigments, as can be seen in Figure 2B. Despite the low DEPS, antenna quenching, which should be mediated by zeaxanthin present in the antenna system, was highest in SD/HT (Fig. 4B). Thus, we propose that exposure of plants to SD/HT induces a higher aggregation state of LHCII, which constitutively quenches excess energy through a zeaxanthin-independent mechanism (Busch et al., 2007). We further propose that this zeaxanthin-independent quenching is due to an increased q_E (the fast-relaxing component of NPQ) mediated by an increase in the pH gradient due to a reduction in CO_2 assimilation rates. This increase in q_E is associated with an increased quantum efficiency for NPQ formation. Increased q_E in SD/HT plants is also indicated by our observation of a very fast relaxation of steady-state fluorescence back to F_0 levels after the actinic light was turned off (Fig. 3).

In addition, under increasing light intensities, violaxanthin is increasingly converted to zeaxanthin, which provides additional photoprotection via zeaxanthin-dependent NPQ. This mechanism seems to be essential especially for LD/LT, which has the highest DEPS across all light intensities as well as the largest xanthophyll pool, providing constitutive quenching. It is generally accepted that a higher amount of zeaxanthin, most efficiently bound to oligomeric LHCII (Johnson et al., 2007), prevents singlet oxygen formation in the antenna (Demmig-Adams and Adams, 2002; Adams et al., 2004). We suggest that under SD/HT conditions, having a very low DEPS, singlet oxygen produced via triplet chlorophyll could be quenched by a higher amount of β-carotene (Fig. 2C), an excellent quencher of singlet oxygen (Cantrell et al., 2003; Krieger-Liszkay, 2005; Telfer, 2005).

Changes in 77 K fluorescence emission characteristics of the long-wavelength peak were observed, and a shift of the emission maximum from 731 nm (LD/HT

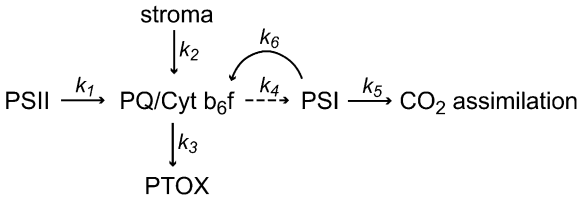

Figure 7. Possible points of regulation for photosynthetic electron transport. k_1 to k_6 indicate rate constants for the flux of electrons. k_4 is highlighted by a dashed line, as this is the probable site of limitation in photosynthetic electron transport. See text for further details.

and SD/HT) to 723 nm (SD/LT) and 713 nm (LD/LT) was detected. Although it has been shown that this could be due to changes in the LHCI composition (Bossmann et al., 1997; Zhang et al., 1997), this is most likely not the case here, since we previously found no significant changes in the relative amount of LHCI components (Busch et al., 2007). We attribute the blue shift to a disconnection of LHCI from PSI, as has been observed previously in iron-deficient *Chlamydomonas* (Moseley et al., 2002), in the red algae *Rhodella violacea* (Desquilbet et al., 2003), and in lincomycin-treated maize (*Zea mays*; Gaspar et al., 2006).

Redox Regulation and Electron Transport under SD/HT Conditions

Plants employ a multiple-step regulation to balance the electron flow with the required rate of ATP and NADPH production under changing environmental conditions. These include D1 turnover, state transitions, NPQ, xanthophyll cycle, chlororespiration, Mehler reaction, cyclic electron flow, and reactive oxygen species production (Scheibe et al., 2005). It has been shown that endogenous systems that measure day-length interact with redox regulation (Becker et al., 2006; Queval et al., 2007). We show, to our knowledge for the first time, that increased temperature under a short, autumn photoperiod (SD/HT) results in higher excitation pressure than in summer control plants (LD/HT; Fig. 4C; i.e. an overreduction of the PQ pool). This appears to be due to limitations in intersystem electron transport and CO_2 assimilation as a consequence of alterations in the structure and composition of the photosynthetic apparatus. PTOX should oxidize an overreduced PQ pool, which should be associated with lower excitation pressure (Rosso et al., 2006). We observed a 3-fold increase in the accumulation of PTOX under SD/HT and low-temperature conditions compared with the summer control plants (LD/HT; Fig. 1G). Although the intersystem electron pool size (e^-/P700) was 44% lower in plants exposed to low temperature (Fig. 5; LD/LT and SD/LT), e^-/P700 was similar in SD/HT compared with LD/HT plants (Fig. 5). Furthermore, excitation pressure, measured as $1 - q_P$, was 1.4-fold higher in SD/HT plants and about 3-fold higher in LD/LT and SD/LT plants than in summer control plants (LD/HT; Fig. 4C). Although PTOX accumulation is stimulated by stress (Fig. 1G), the accumulation of PTOX does not alleviate excitation pressure in *P. banksiana*. Thus, PTOX does not appear to act as a safety valve under conditions of environmental stress in *P. banksiana*, as suggested by Rosso et al. (2006) for Arabidopsis. Alternatively, the higher levels of PTOX may support a higher production of carotenoids by phytoene desaturase in *P. banksiana*. Shahbazi et al. (2007) reported that PTOX is involved in both redox regulation and carotenoid desaturation, in support of the suggestion of Peltier and Cournac (2002). Clearly, the functional role of PTOX remains an enigma.

CONCLUSION

In summary, we have shown that the inhibition of CO_2 assimilation in *P. banksiana* associated with exposure to elevated temperatures during a short, autumn photoperiod is a consequence of an inhibition of photosynthetic electron transport associated with a decreased PSII/PSI stoichiometry coupled with decreased levels of Rubisco. Furthermore, the results presented are consistent with the model for zeaxanthin-independent antenna quenching presented previously (Busch et al., 2007). A major component of photoprotection under a short, autumn photoperiod appears to be antenna quenching through zeaxanthin-independent LHCII aggregation to balance light absorption with a decreased capacity for energy utilization through CO_2 assimilation. In *P. banksiana*, elevated temperatures and a short, autumn photoperiod interact to affect the structure and function of the photosynthetic apparatus, which leads to an inhibition of CO_2 assimilation. The results from our experiments using seedlings grown in controlled environments with a relatively large difference in air temperature do not allow any quantitative prediction of how entire boreal forest stands might be affected by the projected increase of autumn air temperature of 4°C to 7°C by 2100 (ACIA, 2005; IPCC, 2007). However, the experiment clearly demonstrates the significance of warm autumn temperatures on the cold-hardening process in conifers that warrant further investigation (e.g. under manipulated field conditions). A net CO_2 loss in response to autumn warming was recently observed in the field in northern ecosystems, and the underlying mechanisms and processes have yet to be explained (Piao et al., 2008). Models that predict the effects of climate change on conifers of the boreal forests mostly fail to take into account the interactive effects of increased temperatures and short photoperiod (Heimann and Reichstein, 2008). We suggest that the understanding of such an interaction is of critical importance for future modeling of the response of boreal forests of the northern hemisphere to global warming.

MATERIALS AND METHODS

Plant Material and Growth Conditions

One-year-old rooted *Pinus banksiana* (Jack pine) seedlings were obtained from a local nursery (Somerville Seedlings) and planted in a mixture of ProMix (Premier Horticulture) and low-nutrient mineral sand (1:2, v/v). The plants were kept outside underneath a light shelter for 2 years. In the third year, the plants were transferred to controlled environments in late summer 2006 (Conviron growth chambers). Eight 3-year-old plants per treatment were exposed for 4 weeks to either 22°C/18°C (day/night) with a photoperiod of 16 h (LD/HT; representing summer), 22°C/18°C with an 8-h photoperiod (SD/HT; warm autumn conditions), 7°C/5°C with a 16-h photoperiod (LD/LT; cold summer conditions), and 7°C/5°C with an 8-h photoperiod (SD/LT; representing late autumn). The photosynthetic photon flux density was set to 500 μmol photons m^{-2} s^{-1} for all four treatments. Although these light intensity and quality values may not accurately reflect field conditions, a factorial design with temperature and photoperiod as the only two variables allows for a qualitative analysis of the effect of increased autumn air temperature on evergreen conifers.

Protein Extraction, SDS-PAGE, and Immunoblotting

For protein extraction, needles were ground to a fine powder in liquid nitrogen. The proteins were extracted as described in detail previously (Busch et al., 2007). To determine the total concentration of extracted protein, a test after Lowry et al. (1951) was performed, using the RC DC protein assay kit from Bio-Rad. Seven micrograms of protein per lane was loaded and separated electrophoretically at 200 V for 30 min on 10% (w/v) Bis-Tris gels (Nupage; Invitrogen) using the XCell Midi gel system and a MES/SDS buffer system (Invitrogen). The proteins were then transferred to a nitrocellulose membrane (0.2-μm pore size; Bio-Rad) and probed with antibodies against Lhcb1, PsbA, Cyt *f*, PC, and RbcL (Agrisera) as well as against PSI and PTOX. Goat anti-rabbit and rabbit anti-chicken IgG conjugated with horseradish peroxidase (Sigma-Aldrich) were used as secondary antibodies to allow for chemiluminescence detection (ECL detection kit; GE Healthcare) of the proteins bound to the membrane. The membranes treated this way were exposed to x-ray film (Super RX; Fujifilm). The optical density of each band on the film was quantified using the Scion software package (Scion).

Photosynthetic Pigments

Needles of plants of all treatments were detached around noon, when plants had already been exposed to growth light for 4 h. They were then put on trays with their bottom covered with wet filter paper and exposed to 100, 200, 400, 800, and 1,500 μmol photons m^{-2} s^{-1}. After 2 h of exposure to the respective light intensities, the samples were frozen in liquid nitrogen and stored at −80°C until further analysis. In addition, one set of samples was taken in the morning before the light was turned on to get dark-adapted samples. Needles were ground to a fine powder in liquid nitrogen, and pigments were extracted for 2 h in the dark on ice in 100% acetone buffered with $NaHCO_3$. The pigment extracts were separated by HPLC as described (Busch et al., 2007). The deepoxidation state was calculated as DEPS = (0.5A + Z)/(V + A + Z), where A is antheraxanthin, V is violaxanthin, and Z is zeaxanthin.

Chlorophyll Fluorescence Measurements

Chlorophyll *a* fluorescence was measured with a PAM 2100 chlorophyll fluorometer (Heinz Walz). F_0 and F_m (maximum fluorescence) were determined in the morning at the end of the dark period. F_0' (minimal fluorescence immediately after illumination), F_m' (maximum fluorescence under actinic light), and F_t (transient fluorescence) were recorded after steady-state fluorescence was achieved, usually within a 3-min illumination period. Optimum quantum efficiency of PSII was calculated as $F_v/F_m = (F_m - F_0)/F_m$, and the effective quantum yield of PSII in the light was calculated as $F_v'/F_m' = (F_m' - F_t)/F_m'$ (Genty et al., 1989). The fraction of PSII reaction centers in a closed state was estimated as $1 - q_P = 1 - (F_m' - F_t)/(F_m' - F_0')$ (Schreiber and Bilger, 1987). NPQ was calculated as $F_m/F_m' - 1$ (Bilger and Björkman, 1990), and antenna quenching was calculated as $q_0 = 1 - F_0'/F_0$, according to Rees et al. (1990).

To assess the relaxation of F_0 quenching, the plants were dark adapted for 20 min with a dark leaf clip and subsequently exposed to 650 μmol photons m^{-2} s^{-1} for 4.5 min. The postillumination relaxation of chlorophyll fluorescence was followed at the F_0' level after switching off the actinic light with and without simultaneously applying FR light.

P700 Measurements

The redox state of P700 was determined in vivo using a PAM-101 modulated chlorophyll fluorometer (Heinz Walz) equipped with an ED-P700DW detector following the procedure of Schreiber et al. (1988), as described in detail by Ivanov et al. (1998). FR light (λ_{max} = 715 nm, 10 W m^{-2}; Schott filter RG 715) was provided by the 101 FR light source. Multiple-turnover (50 ms) and single-turnover (half-peak width, 14 μs) saturating flashes were applied with the Walz XMT-103 power unit and the Walz XST-103 control unit. The redox state of P700 was measured on detached needles as the $\Delta A_{820}/A_{820}$ at growth temperature (22°C or 7°C). The transient reduction of $P700^+$ signal after application of single- and multiple-turnover flashes of white saturating light was used to estimate the intersystem electron pool size (Asada et al., 1993; Ivanov et al., 1998).

Low-Temperature Fluorescence Measurements

Low-temperature (77 K) chlorophyll fluorescence emission spectra were collected using a PTI QM-7/2006 spectrofluorometer (Photon Technology International) equipped with a double monochromator, R928P red-sensitive photomultiplier tube (Hamamatsu Photonics) and a liquid nitrogen device. Thylakoid membranes suspended in a buffer containing 35 mM Tricine (pH 7.8), 0.3 M sorbitol, 7 mM NaCl, and 3.5 mM $MgCl_2$ were dark adapted for 30 min and frozen in the presence of 30% glycerol before the measurements. The chlorophyll concentration was 5 μg mL^{-1}. Corrected fluorescence emission spectra were excited at 436 nm and recorded from 650 to 800 nm using a slit width of 2.5 nm for both excitation and emission. All fluorescence spectra were additionally corrected by subtracting the medium blank.

Statistics

The effects of daylength and temperature on photosynthetic properties were statistically analyzed by two-way ANOVA at $P < 0.05$ using SPSS version 14.0. All significant differences mentioned in the text and the figures refer to the two-way ANOVA results.

ACKNOWLEDGMENTS

We are grateful to Dr. P.E. Jensen (Royal Veterinary and Agricultural University, Copenhagen) for providing the PSI antibody. We thank Marc Possmayer (University of Western Ontario, London, Canada) for assisting with the data collection.

Received February 9, 2008; accepted March 18, 2008; published March 28, 2008.

LITERATURE CITED

ACIA (2005) Arctic Climate Impact Assessment. Cambridge University Press, Cambridge, UK

Adams WW, Zarter CR, Ebbert V, Demmig-Adams B (2004) Photoprotective strategies of overwintering evergreens. Bioscience **54:** 41–49

Albertsson PA (2001) A quantitative model of the domain structure of the photosynthetic membrane. Trends Plant Sci **6:** 349–354

Asada K (1999) The water-water cycle in chloroplasts: scavenging of active oxygens and dissipation of excess photons. Annu Rev Plant Physiol Plant Mol Biol **50:** 601–639

Asada K (2000) The water-water cycle as alternative photon and electron sinks. Philos Trans R Soc Lond B Biol Sci **355:** 1419–1430

Asada K, Heber U, Schreiber U (1993) Electron flow to the intersystem chain from stromal components and cyclic electron flow in maize chloroplasts, as detected in intact leaves by monitoring redox change of P700 and chlorophyll fluorescence. Plant Cell Physiol **34:** 39–50

Beck EH, Heim R, Hansen J (2004) Plant resistance to cold stress: mechanisms and environmental signals triggering frost hardening and dehardening. J Biosci **29:** 449–459

Becker B, Holtgrefe S, Jung S, Wunrau C, Kandlbinder A, Baier M, Dietz KJ, Backhausen JE, Scheibe R (2006) Influence of the photoperiod on redox regulation and stress responses in *Arabidopsis thaliana* L. (Heynh.) plants under long- and short-day conditions. Planta **224:** 380–393

Bigras FJ, Ryyppö A, Lindström A, Stattin E (2001) Cold acclimation and deacclimation of shoots and roots of conifer seedlings. *In* FJ Bigras, SJ Colombo, eds, Conifer Cold Hardiness. Kluwer Academic Publishers, Dordrecht, The Netherlands, pp 57–88

Bilger W, Björkman O (1990) Role of the xanthophyll cycle in photoprotection elucidated by measurements of light-induced absorbency changes, fluorescence and photosynthesis in leaves of *Hedera canariensis.* Photosynth Res **25:** 173–185

Bossmann B, Knoetzel J, Jansson S (1997) Screening of chlorina mutants of barley (*Hordeum vulgare* L.) with antibodies against light-harvesting proteins of PS I and PS II: absence of specific antenna proteins. Photosynth Res **52:** 127–136

Busch F, Hüner NPA, Ensminger I (2007) Increased air temperature during simulated autumn conditions does not increase photosynthetic carbon gain but affects the dissipation of excess energy in seedlings of the evergreen conifer Jack pine. Plant Physiol **143:** 1242–1251

Cantrell A, McGarvey DJ, Truscott TG, Rancan F, Bohm F (2003) Singlet oxygen quenching by dietary carotenoids in a model membrane environment. Arch Biochem Biophys **412:** 47–54

Carol P, Stevenson D, Bisanz C, Breitenbach J, Sandmann G, Mache R, Coupland G, Kuntz M (1999) Mutations in the *Arabidopsis* gene immutans cause a variegated phenotype by inactivating a chloroplast terminal oxidase associated with phytoene desaturation. Plant Cell **11:** 57–68

Christersson L (1978) The influence of photoperiod and temperature on the development of frost hardiness in seedlings of *Pinus silvestris* and *Picea abies*. Physiol Plant **44:** 288–294

Cruz JA, Salbilla BA, Kanazawa A, Kramer DM (2001) Inhibition of plastocyanin to P_{700}^{+} electron transfer in *Chlamydomonas reinhardtii* by hyperosmotic stress. Plant Physiol **127:** 1167–1179

Demmig-Adams B, Adams WW (2002) Antioxidants in photosynthesis and human nutrition. Science **298:** 2149–2153

Demmig-Adams B, Gilmore AM, Adams WW (1996) Carotenoids 3. In vivo functions of carotenoids in higher plants. FASEB J **10:** 403–412

Desquilbet TE, Duval JC, Robert B, Houmard J, Thomas JC (2003) In the unicellular red alga *Rhodella violacea* iron deficiency induces an accumulation of uncoupled LHC. Plant Cell Physiol **44:** 1141–1151

Ensminger I, Busch F, Hüner NPA (2006) Photostasis and cold acclimation: sensing low temperature through photosynthesis. Physiol Plant **126:** 28–44

Ensminger I, Schmidt L, Lloyd J (2008) Soil temperature and intermittent frost modulate the rate of recovery of photosynthesis in Scots pine under simulated spring conditions. New Phytol **177:** 428–442

Ensminger I, Sveshnikov D, Campbell DA, Funk C, Jansson S, Lloyd J, Shibistova O, Öquist G (2004) Intermittent low temperatures constrain spring recovery of photosynthesis in boreal Scots pine forests. Glob Change Biol **10:** 995–1008

Gaspar L, Sarvari E, Morales F, Szigeti Z (2006) Presence of 'PSI free' LHCI and monomeric LHCII and subsequent effects on fluorescence characteristics in lincomycin treated maize. Planta **223:** 1047–1057

Genty B, Briantais JM, Baker NR (1989) The relationship between the quantum yield of photosynthetic electron-transport and quenching of chlorophyll fluorescence. Biochim Biophys Acta **990:** 87–92

Golding AJ, Johnson GN (2003) Down-regulation of linear and activation of cyclic electron transport during drought. Planta **218:** 107–114

Haehnel W (1984) Photosynthetic electron transport in higher plants. Annu Rev Plant Physiol Plant Mol Biol **35:** 659–693

Heimann M, Reichstein M (2008) Terrestrial ecosystem carbon dynamics and climate feedbacks. Nature **451:** 289–292

Horton P, Wentworth M, Ruban A (2005) Control of the light harvesting function of chloroplast membranes: the LHCII-aggregation model for non-photochemical quenching. FEBS Lett **579:** 4201–4206

Huner NPA, Öquist G, Sarhan F (1998) Energy balance and acclimation to light and cold. Trends Plant Sci **3:** 224–230

IPCC (2007) Climate Change 2007: The Physical Science Basis. Contribution of Working Group I to the Fourth Assessment Report of the Intergovernmental Panel on Climate Change. Cambridge University Press, Cambridge, UK

Ivanov AG, Morgan RM, Gray GR, Velitchkova MY, Huner NPA (1998) Temperature/light dependent development of selective resistance to photoinhibition of photosystem I. FEBS Lett **430:** 288–292

Johnson MP, Havaux M, Triantaphylides C, Ksas B, Pascal AA, Robert B, Davison PA, Ruban AV, Horton P (2007) Elevated zeaxanthin bound to oligomeric LHCII enhances the resistance of Arabidopsis to photooxidative stress by a lipid-protective, antioxidant mechanism. J Biol Chem **282:** 22605–22618

Kirchhoff H, Schöttler MA, Maurer J, Weis E (2004) Plastocyanin redox kinetics in spinach chloroplasts: evidence for disequilibrium in the high potential chain. Biochim Biophys Acta **1659:** 63–72

Klimov SV (2003) Cold hardening of plants is a result of maintenance of an increased photosynthesis/respiration ratio at low temperatures. Biol Bull **30:** 48–52

Klughammer C, Schreiber U (1991) Analysis of light-induced absorbency changes in the near-infrared spectral region. 1. Characterization of various components in isolated chloroplasts. Z Naturforsch [C] **46:** 233–244

Krause GH, Weis E (1991) Chlorophyll fluorescence and photosynthesis: the basics. Annu Rev Plant Physiol Plant Mol Biol **42:** 313–349

Krieger-Liszkay A (2005) Singlet oxygen production in photosynthesis. J Exp Bot **56:** 337–346

Li CY, Puhakainen T, Welling A, Vihera-Aarnio A, Ernstsen A, Junttila O, Heino P, Pavla ET (2002) Cold acclimation in silver birch (*Betula pendula*). Development of freezing tolerance in different tissues and climatic ecotypes. Physiol Plant **116:** 478–488

Lowry OH, Rosebrough NJ, Farr AL, Randall RJ (1951) Protein measurement with the Folin phenol reagent. J Biol Chem **193:** 265–275

Maxwell PC, Biggins J (1976) Role of cyclic electron transport in photosynthesis as measured by the photoinduced turnover of P_{700} in vivo. Biochemistry **15:** 3975–3981

Moseley JL, Allinger T, Herzog S, Hoerth P, Wehinger E, Merchant S, Hippler M (2002) Adaptation to Fe-deficiency requires remodeling of the photosynthetic apparatus. EMBO J **21:** 6709–6720

Müller P, Li XP, Niyogi KK (2001) Non-photochemical quenching : a response to excess light energy. Plant Physiol **125:** 1558–1566

Öquist G, Huner NPA (2003) Photosynthesis of overwintering evergreen plants. Annu Rev Plant Biol **54:** 329–355

Peltier G, Cournac L (2002) Chlororespiration. Annu Rev Plant Biol **53:** 523–550

Piao SL, Ciais P, Friedlingstein P, Peylin P, Reichstein M, Luyssaert S, Margolis H, Fang JY, Barr A, Chen AP, et al (2008) Net carbon dioxide losses of northern ecosystems in response to autumn warming. Nature **451:** 49–53

Puhakainen T, Li CY, Boije-Malm M, Kangasjarvi J, Heino P, Palva ET (2004) Short-day potentiation of low temperature-induced gene expression of a C-repeat-binding factor-controlled gene during cold acclimation in silver birch. Plant Physiol **136:** 4299–4307

Queval G, Issakidis-Bourguet E, Hoeberichts FA, Vandorpe M, Gakiere B, Vanacker H, Miginiac-Maslow M, Van Breusegem F, Noctor G (2007) Conditional oxidative stress responses in the Arabidopsis photorespiratory mutant cat2 demonstrate that redox state is a key modulator of daylength-dependent gene expression, and define photoperiod as a crucial factor in the regulation of H_2O_2-induced cell death. Plant J **52:** 640–657

Quiles MJ (2006) Stimulation of chlororespiration by heat and high light intensity in oat plants. Plant Cell Environ **29:** 1463–1470

Rees D, Noctor GD, Horton P (1990) The effect of high-energy-state excitation quenching on maximum and dark level chlorophyll fluorescence yield. Photosynth Res **25:** 199–211

Rosso D, Ivanov AG, Fu A, Geisler-Lee J, Hendrickson L, Geisler M, Stewart G, Krol M, Hurry V, Rodermel SR, et al (2006) IMMUTANS does not act as a stress-induced safety valve in the protection of the photosynthetic apparatus of Arabidopsis during steady-state photosynthesis. Plant Physiol **142:** 574–585

Rumeau D, Peltier G, Cournac L (2007) Chlororespiration and cyclic electron flow around PSI during photosynthesis and plant stress response. Plant Cell Environ **30:** 1041–1051

Saxe H, Cannell MGR, Johnsen B, Ryan MG, Vourlitis G (2001) Tree and forest functioning in response to global warming. New Phytol **149:** 369–399

Scheibe R, Backhausen JE, Emmerlich V, Holtgrefe S (2005) Strategies to maintain redox homeostasis during photosynthesis under changing conditions. J Exp Bot **56:** 1481–1489

Schöttler MA, Kirchhoff H, Weis E (2004) The role of plastocyanin in the adjustment of the photosynthetic electron transport to the carbon metabolism in tobacco. Plant Physiol **136:** 4265–4274

Schreiber U, Bilger W (1987) Rapid assessment of stress effects on plant leaves by chlorophyll fluorescence measurements. *In* JD Tenhunen, FM Catarino, OL Lange, WC Oechel, eds, Plant Response to Stress: Functional Analysis in Mediterranean Ecosystems, Vol 15. NATO Advanced Science Institute Series, Berlin, pp 27–53

Schreiber U, Klughammer C, Neubauer C (1988) Measuring P700 absorbance changes around 830 nm with a new type of pulse-modulation system. Z Naturforsch [C] **43:** 686–698

Shahbazi M, Gilbert M, Labouré A, Kuntz M (2007) The dual role of the plastid terminal oxidase (PTOX) in tomato. Plant Physiol **145:** 691–702

Slot M, Wirth C, Schumacher J, Mohren GMJ, Shibistova O, Lloyd J, Ensminger I (2005) Regeneration patterns in boreal Scots pine glades linked to cold-induced photoinhibition. Tree Physiol **25:** 1139–1150

Streb P, Josse EM, Gallouet E, Baptist F, Kuntz M, Cornic G (2005) Evidence for alternative electron sinks to photosynthetic carbon assim-

ilation in the high mountain plant species *Ranunculus glacialis*. Plant Cell Environ **28:** 1123–1135

Sveshnikov D, Ensminger I, Ivanov AG, Campbell D, Lloyd J, Funk C, Hüner NPA, Öquist G (2006) Excitation energy partitioning and quenching during cold acclimation in Scots pine. Tree Physiol **26:** 325–336

Telfer A (2005) Too much light? How beta-carotene protects the photosystem II reaction centre. Photochem Photobiol Sci **4:** 950–956

Vandorssen RJ, Plijter JJ, Dekker JP, Denouden A, Amesz J, Vangorkom HJ (1987) Spectroscopic properties of chloroplast grana membranes and of the core of photosystem-II. Biochim Biophys Acta **890:** 134–143

Wakasugi T, Tsudzuki J, Ito S, Nakashima K, Tsudzuki T, Sugiura M (1994) Loss of all Ndh genes as determined by sequencing the entire chloroplast genome of the black pine *Pinus thunbergii*. Proc Natl Acad Sci USA **91:** 9794–9798

Weiser CJ (1970) Cold resistance and injury in woody plants: Knowledge of hardy plant adaptations to freezing stress may help us to reduce winter damage. Science **169:** 1269–1278

Wentworth M, Ruban AV, Horton P (2004) The functional significance of the monomeric and trimeric states of the photosystem II light harvesting complexes. Biochemistry **43:** 501–509

White A, Cannell MGR, Friend AD (2000) The high-latitude terrestrial carbon sink: a model analysis. Glob Change Biol **6:** 227–245

Wingler A, Lea PJ, Quick WP, Leegood RC (2000) Photorespiration: metabolic pathways and their role in stress protection. Philos Trans R Soc Lond B Biol Sci **355:** 1517–1529

Zhang H, Goodman HM, Jansson S (1997) Antisense inhibition of the photosystem I antenna protein Lhca4 in *Arabidopsis thaliana*. Plant Physiol **115:** 1525–1531